LAWRENCE
LIVERMORE
NATIONAL
LABORATORY

LLNL-JRNL-641356

Experimental determination of gamma-ray discrimination in pillar-structured thermal neutron detectors under high gamma-ray flux

Q. Shao, A. M. Conway, L. F. Voss, R. P. Radev, R. J. Nikolic, M. A. Dar, C. L. Cheung

July 24, 2013

Nuclear Instruments and Methods in Physics Research A

Disclaimer

Experimental Determination of Gamma-ray Discrimination in Pillar-structured Thermal Neutron Detectors under High Gamma-ray Flux

Qinghui Shao[a], Adam M. Conway[a], Lars F. Voss[a], Radoslav P. Radev[a], Rebecca J. Nikolić[a,*], Mushtaq A. Dar[b], and Chin L. Cheung[c]

[a]Lawrence Livermore National Laboratory, 7000 East Ave., Livermore, CA 94550, USA

[b]King Saud University, Riyadh 11421 Kingdom of Saudi Arabia

[c]Department of Chemistry, University of Nebraska-Lincoln, Lincoln, NE 68588, USA

[*]Corresponding author. E-mail address: nikolic1@llnl.gov

Abstract

Silicon pillar structures filled with a neutron converter material (^{10}B) are designed to have high thermal neutron detection efficiency with specific dimensions of 50 μm pillar height, 2 μm pillar diameter and 2 μm spacing between adjacent pillars. In this paper, we have demonstrated such a detector has a high neutron-to-gamma discrimination of 10^6 with a high thermal neutron detection efficiency of 39% when exposed to a high gamma-ray field of 10^9 photons/cm^{2}s.

Keywords

Thermal neutron detector, Gamma-ray discrimination, Silicon pillar, Boron

Hellium-3 tubes are the most widely used technology for detecting neutrons due to their high neutron detection efficiency as well as low gamma-ray sensitivity, but there are issues with stability, sensitivity to microphonics, and very recently a shortage of hellium-3 [1]. In order to find alternatives, solid-state thermal neutron detectors have been investigated that utilize various architectures and material combinations [2-7]. Many solid-state thermal neutron detectors are more sensitive to gamma-rays compared to helium-3 tubes, which is compounded by the fact that most nuclear materials emit 10 or more times as many gamma-rays as neutrons. For measurements of spent fuel, where gamma-ray fluxes of 1000 R/h (~ 10^9 photons/cm^{2}s) or more

are encountered, the gamma-ray sensitivity of the detector may dominate all other considerations [8]. The electronic pulses generated by gamma-rays can be readily rejected by setting a high low-level-discriminator (LLD). However, a high LLD setting will limit the registration of low-energy pulses created by neutron events. The gamma-ray insensitivity and intrinsic neutron detection efficiency are therefore important figures-of-merit for evaluating the performance of a neutron detector. In this paper, we report superior performance of thermal neutron detection and gamma-ray discrimination of a pillar detector under a high gamma-ray flux environment (up to 10^9 photons/cm^{2}s).

^{10}B is selected as the neutron converter material in our devices because of its high thermal neutron cross section of 3840 barns, compared to 940 barns of ^{6}Li, which is also a popular neutron converter in solid-state thermal neutron detectors [2-3]. The thermal neutron capture reaction by ^{10}B can be described as follows [9]:

$$ {}^{10}_{5}B + {}^{1}_{0}n \rightarrow \begin{cases} {}^{7}_{3}Li(1.015MeV) + {}^{4}_{2}\alpha(1.777MeV) \ \ (ground\,state, 6\%) \\ {}^{7}_{3}Li^{*}(0.84MeV) + {}^{4}_{2}\alpha(1.47MeV) \ \ (1^{st}\,excited\,state, 94\%) \end{cases} \quad (1) $$

The reaction byproducts deposit their energy into the semiconductor and generate electron-hole pairs. The charge carriers are swept out by an internal or applied electric field and collected by the electrodes for the registration of a neutron event. The selected semiconductor material should have a relative low atomic number (Z) and density (ρ) for the purpose of low gamma-ray interaction [9]. Silicon is used in our pillar detectors, because it has both a low Z of 14 and ρ of 2.33 g/cm^3. Murphy *et al*. reported that Si provides better gamma-ray rejection compared with other semiconductor materials, *i.e.,* C (diamond), ZnO, GaAs, and CdTe [10].

Our Si-^{10}B detector design is based on using a three-dimensionally integrated approach. Figure 1 (a) shows a schematic of a pillar structured thermal neutron detector. A silicon wafer comprised of a 3 μm p^+ layer and a 47 μm intrinsic layer (n^-) epitaxially grown on an n^+ substrate was used for device fabrication. The pillar diameter and spacing were defined lithographically, followed by deep reactive ion etching to form a 50-μm-tall pillar array. A conformal ^{10}B coating was deposited to fill the gaps in the pillar array by chemical vapor deposition [11]. A Plasma Quest electron cyclotron resonance etcher was used for boron etching on the front side to expose the

highly conductive p^+ pillar tops as shown in Fig. 1 (b). This was followed by surface planarization using Honeywell Accuflo™ 2027 spin-on-polymer and chemical mechanical polishing. Finally the stacking layers of Al/Cr/Au, 5000Å/500Å/7500Å were sputtered on both sides for metal contacts. The geometrical constraints on the converter material thickness are decoupled from the limitation of the ion track length [4-7]. The ^{10}B thickness is defined by the pillar height, and is three times the mean free path of thermal neutrons in ^{10}B which is ~ 50 µm. The pillar pitch of 4 µm (2 µm pillar diameter and 2 µm pillar spacing) is designed to allow a high probability of interaction between the energetic ions and the semiconductor pillars, created by nuclear reaction of the neutron with ^{10}B [4]. When the pillar height and pitch are optimized high thermal neutron detection efficiency (~ 50%) and high neutron-to-gamma-ray discrimination (> 10^5) are predicted [4].

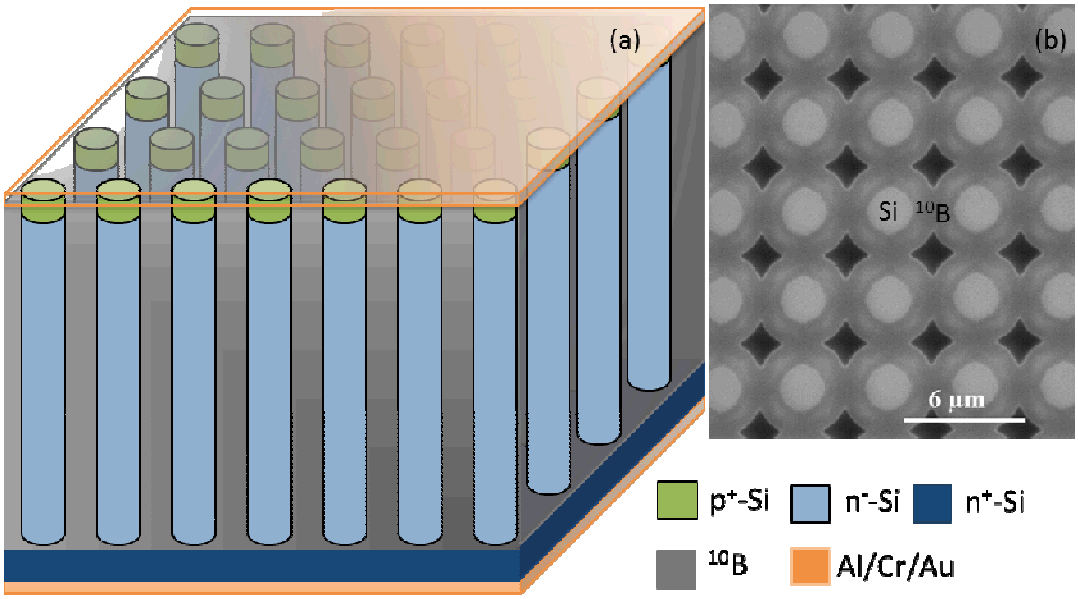

Fig. 1 (a) Schematic of a pillar structured solid-state thermal neutron detector with 2 µm pillar diameter, 2 µm pillar spacing and 50 µm pillar height (the dimensions are not to scale), and (b) scanning electron microscopy image of boron filled pillar arrays (top view).

In the pillar detector shown in Fig. 1, neutron absorption only takes place in the neutron conversion material (^{10}B), which is defined by the pillar height. Gamma-ray interaction, on the other hand, takes place in the entire Si portion. Previously we investigated the effect of the intrinsic layer below the pillars on gamma-ray sensitivity in a structure with a 25 µm intrinsic

layer. We found that the lowest gamma-ray response occurs when the thickness of intrinsic region below the pillars is reduced to a minimum due to less gamma-silicon interaction in the active region. This is the region in our structure where the generated electron hole pairs can be collected [6]. Thus it is important to select a starting layer structure where the intrinsic layer thickness is close to the designed pillar height. In this paper, the pillars of the device under test were formed by etching completely through the intrinsic region to reduce the gamma-ray sensitivity.

The photograph of the experimental setup is shown in the inset of Fig. 2. A detector with 2×2 mm^2 total area composed of a 50-μm-tall pillar array (see Fig. 1) was attached to a side of a 5 cm-thick high-density polyethylene moderation fixture where inserted was a ^{252}Cf source which emits fission neutrons. The high-density polyethylene fixture moderates the high energy neutrons to produce thermal neutrons (~ 0.025 eV). The thermal neutron flux on the detector surface was constant under all test conditions at ~ 48 n/cm^2s obtained by modeling using MCNP and folding the simulated spectrum with the ^{10}B cross section [7]. The fixture sat on a moving cart which controls the gamma-ray flux striking on the detector surface by varying the distance of the detector from the gamma-ray source: ^{137}Cs with activity of 218.2 Ci. An ORTEC 142C preamplifier, ORTEC 572 shaping amplifier, and ORTEC AMETEK EASY-MCA-2K multichannel analyzer were used for data acquisition. A shaping time of 0.5 μs and a measurement live time of 20 minutes were used.

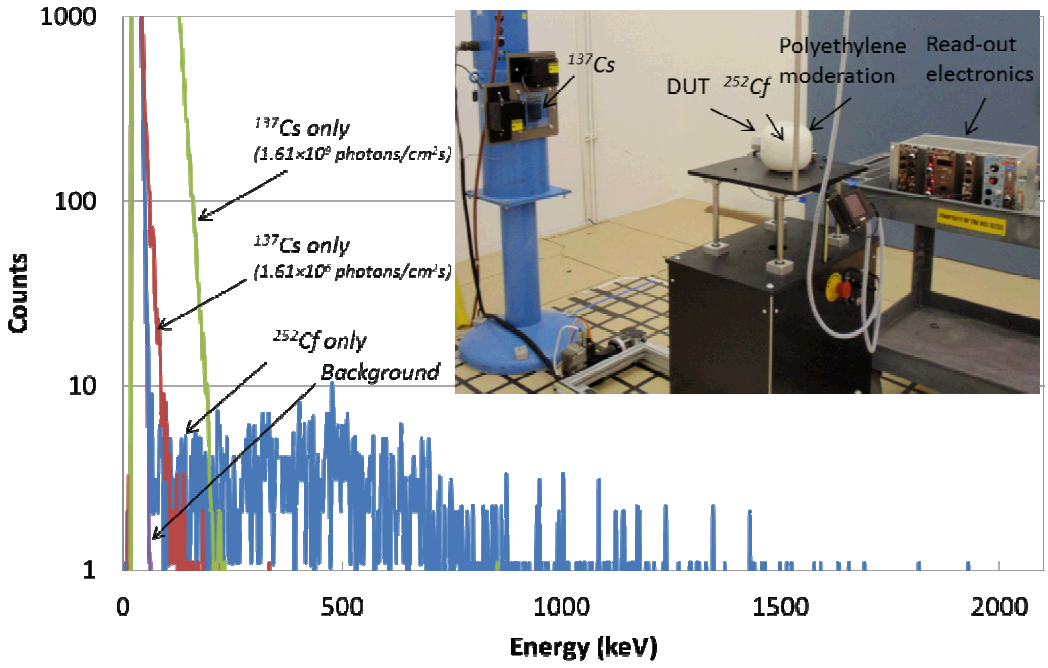

Fig. 2 Measured background spectrum (no source), neutron detection spectrum and gamma detection spectrum of a 2 × 2 mm^2 50-μm-tall pillar detector using the geometry shown in Fig. 1. ^{137}Cs and ^{252}Cf were used as gamma-ray source and neutron source, respectively. The inset shows a photograph of the measurement setup.

Fig. 2 shows the measured neutron detection spectrum with ^{252}Cf and gamma detection spectrum with ^{137}Cs of a 2 × 2 mm^2 pillar detector using the geometry shown in Fig. 1. The gamma-ray fluxes on the detector surface in the measurements were 1.61 × 10^6 and 1.61 × 10^9 photons/cm^2s obtained by positioning the detector at distance of 632 cm and 20 cm away from the gamma-ray source respectively. The intrinsic thermal neutron detection efficiency ($\varepsilon_{int\,n}$) is defined by dividing the number of counted neutrons in the neutron spectra by the number of thermal neutrons incident on the 2 × 2 mm^2 detector. Analogously, the intrinsic gamma-neutron detection efficiency ($\varepsilon_{int\,\gamma n}$) is defined by dividing the number of counted gamma-rays by the number of gamma-rays incident on the detector. Thus we obtained the neutron to gamma-ray discrimination (n/γ):

$$n/\gamma = \varepsilon_{\mathrm{int}\,n} / \varepsilon_{\mathrm{int}\gamma n} \qquad (2)$$

The relationship between $\varepsilon_{int\,n}$, n/γ discrimination and the LLD settings is shown in Fig. 3. Within the LLD range of 67 to 107 keV, the two n/γ discrimination curves are close and they increase greatly from 9×10^4 to 9×10^5 (gamma-ray flux: 1.61×10^6 photons/cm^{2}s) and 5.4×10^4 to 1×10^6 (gamma-ray flux: 1.61×10^9 photons/cm^{2}s), while the thermal neutron detection efficiency only decreases slightly from 41.0% to 38.9%.

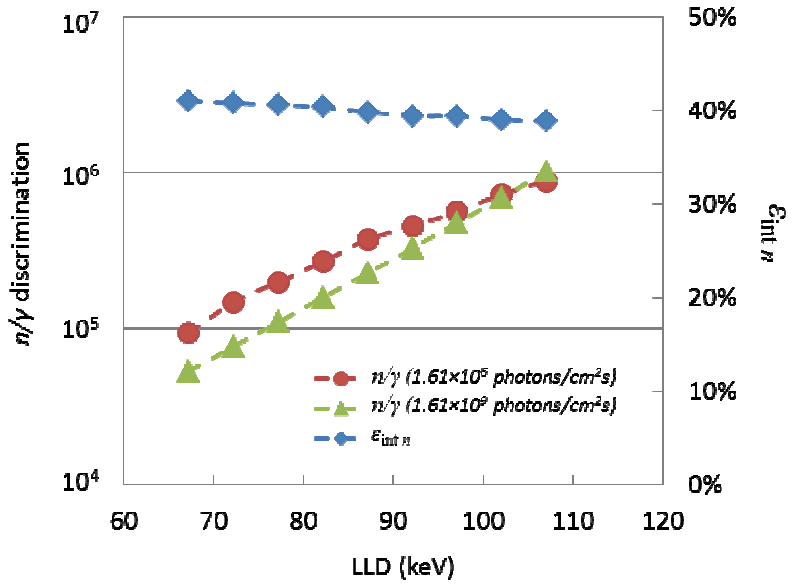

Fig. 3 Measured thermal neutron detection efficiency without a gamma-ray source and n/γ discrimination as a function of LLD with gamma-ray fluxes of 10^6 and 10^9 photons/cm^{2}s.

The gamma-ray insensitivity of neutron detectors in Radiation Portal Monitor (RPM) systems for homeland security applications requires that gamma radiation at exposure rate of up to 10 mR/h shall not trigger the neutron alarm as defined in American National Standards Institute ANSI N 42.35-2006 [12]. As a benchmark, we set a goal of gamma-ray insensitivity of $\varepsilon_{int\,\gamma n} \leq 10^{-6}$ in the presence of a ^{137}Cs source at exposure rate greater than 10 mR/h [13]. The LLD of 95 keV is selected to ensure $\varepsilon_{int\gamma n} \leq 10^{-6}$. The corresponding intrinsic thermal neutron detection efficiency is 39.4% and n/γ discriminations are 5.3×10^5 (gamma-ray flux: 1.61×10^6 photons/cm^{2}s) and 4×10^5 (gamma-ray flux: 1.61×10^9 photons/cm^{2}s). The measured n/γ discriminations are consistent with MCNP simulation results which are on the order of 10^5 based on the same device structure [4]. Note that the gamma-ray flux converted from the exposure rate of 10 mR/h is on

the order of 10^4 photons/cm^{2}s [9], which is much lower than what we had in the experiment.

For a 2.5 × 2.5 mm^2 ^{10}B-Si honeycomb structured thermal neutron detector exposed to a ^{60}Co gamma-ray source with rate of 10 mR/h, an *n/γ* discrimination of 2.4×10^4 was obtained given by the reported thermal neutron detection efficiency of 26.1% and gamma sensitivity (intrinsic gamma-neutron detection efficiency) of 1.1×10^{-5} [14, 15]. As the hexagonal hole depth (45 μm) in the honeycomb structure is close to the pillar height (50 μm), a higher *n/γ* discrimination of 10^6 in the pillar detector could mainly be attributed to a relatively smaller Si volume portion of 20% in the active region compared to 46% in a honeycomb structure designed with 2.8 μm hole diameter and 1 μm Si wall thickness [14-16]. In ^{6}LiF based thermal neutron detectors, due to its relatively low thermal neutron cross section, the active region is usually greater than 250 μm for sufficient neutron absorption. Therefore they have much larger intrinsic Si portions, which are sensitive to the gamma-rays. A high LLD is set in order to reject them. In back-to-back stacking of 1cm^2 ^{6}LiF –Si detectors, an *n/γ* discrimination of 2.2×10^4 with a LLD of 300 keV and 1.0×10^6 with a higher LLD of 450 keV were obtained using ^{137}Cs as gamma-ray source with a flux of 8.6×10^4 photons/cm^{2}s reported by S. L. Bellinger *et al.* [17].

The neutron performance of the 50-μm-tall pillar detector in a high gamma-ray environment was investigated with the presence of both a ^{252}Cf source and a ^{137}Cs source. By moving the detector closer to the ^{137}Cs source, the obtained gamma-ray fluxes were 1.61×10^6, 1.61×10^7, 1.61×10^8, and 1.61×10^9 photons/cm^{2}s at distances of 632 cm, 200 cm, 63.2 cm, and 20 cm respectively. The measured pulse height spectra are shown in Figure 4. The total measured neutron counts above LLD are in the range of 802 to 947. As the gamma-ray flux increases there is more than one gamma-ray striking the detector within the resolving time of the system, thus the electronic pulse amplitude is the sum of the separate events (gamma-ray pile-up). As a result, a high energy pulse is registered into the system. To accommodate the high count rate, the shortest available shaping time of 0.5 μs in ORTEC 572 shaping amplifier is used. Applying a reverse bias voltage can reduce charge collection time by a high electrical field in the Si pillars. However it also causes a high noise level associated with leakage current which negatively affects the neutron detection performance by increasing the noise. Therefore a reversed bias was not applied to the detector.

To reject the pile-up gamma-ray pulses, the LLD is set higher than 62 keV which is the LLD setting with no gamma-ray source present, therefore some neutron counts are lost. The "gamma-ray absolute rejection ratio for neutrons" (GARRn) is defined in PNNL report which measures the detector response in the presence of both a large gamma-ray source and a ^{252}Cf neutron source [13]. The GARRn value will be unity if the gamma-ray source has no impact. To meet the GARRn requirement of $0.9 \leq \text{GARRn} \leq 1.1$ at 10 mR/h exposure, the LLD are set to 95 keV, 105 keV, 134 keV and 182 keV for the gamma-ray flux of 1.61×10^6, 1.61×10^7, 1.61×10^8, and 1.61×10^9 respectively.

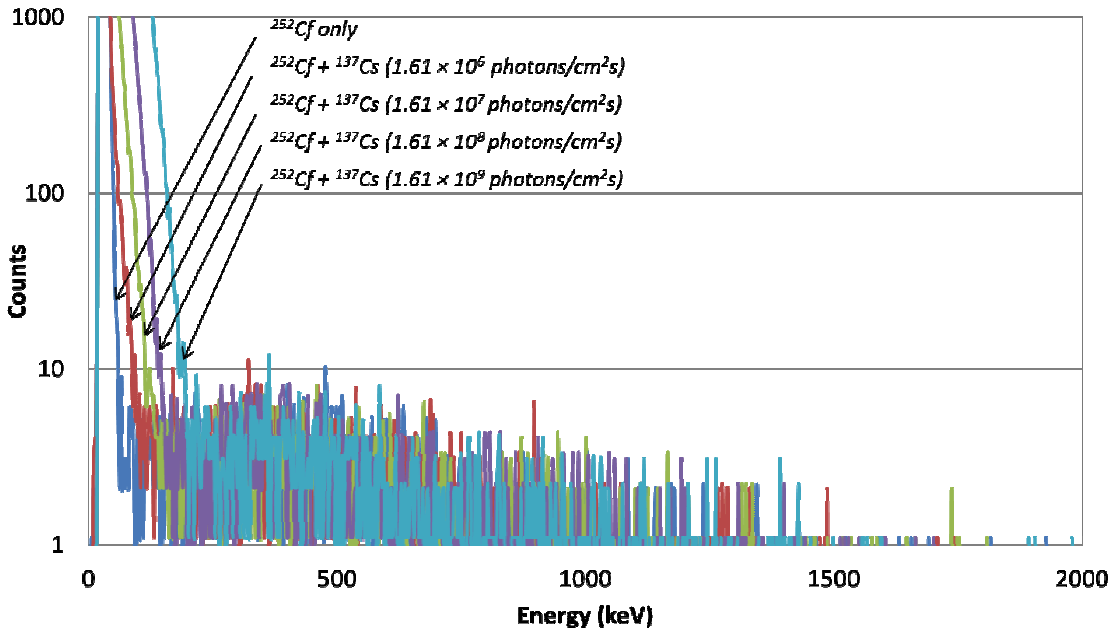

Fig. 4 Pulse height spectra of a 2×2 mm^2 50-µm-tall pillar detector using the geometry shown in Fig. 1 exposed to a ^{252}Cf source and ^{137}Cs source with varied fluxes. The gamma-ray fluxes are shown in parentheses.

To measure the lost portion of neutron events due to the high LLD settings, the neutron count rates are normalized to the 62 keV LLD setting based on the measured neutron response spectra shown in Fig. 2. The neutron count rate drops with an increased gamma-ray flux because a higher LLD is required (Fig. 5). At the gamma-ray flux of 1.61×10^6 photons/cm^{2}s, a normalized neutron count rate of 0.95 with an LLD of 95 keV was obtained, which means 5% of neutron counts is lost. As the gamma-ray flux increases to 1.61×10^9 photons/cm^{2}s, the normalized

neutron count rate drops to 0.85 with an LLD of 182 keV, which corresponds to a 15% reduction in the neutron counts, and a thermal neutron detection efficiency of 35% is maintained when the detector is exposed to such a high gamma-ray flux field.

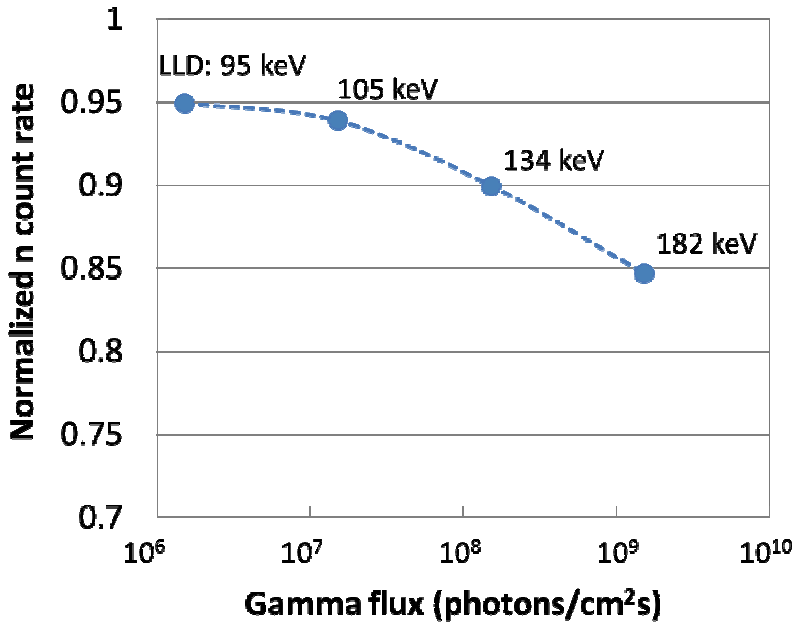

Fig. 5 Neutron count rates normalized to the 62 keV LLD with no gamma-ray source present, measured with a 2 × 2 mm^2 50-μm-tall pillar detector using the geometry shown in Fig.1. The LLDs are set based on incident gamma-ray fluxes to meet the requirement: 0.9 ≤ GARRn ≤ 1.1.

We have demonstrated that a pillar structured thermal neutron detector based on a Si-^{10}B composite can simultaneously achieve a high thermal neutron detection efficiency of 39% as well as a high *n/γ* discrimination of 10^6 in a high gamma-ray field of 10^9 photons/cm^2s because of the small overall Si volume in the active region. While tuning the LLD to meet the gamma-ray insensitivity requirement: 0.9 ≤ GARRn ≤ 1.1 a thermal neutron detection efficiency of 35% is maintained.

The authors would like to acknowledge Tim Graff and Cathy Reinhardt for their excellent support in the clean room fabrication. This work was performed under the auspices of the U.S. Department of Energy by Lawrence Livermore National Laboratory under Contract No. DE-

AC52-07NA27344, LLNL-JRNL-641356. This work has been supported by the US Department of Homeland Security, Domestic Nuclear Detection Office, under competitively awarded IAA HSHQDC-08-X-00874. This support does not constitute an express or implied endorsement on the part of the government.

References

[1] R. T. Kouzes, "The ^{3}He supply problem," Pacific Northwest National Laboratory Report PNNL-18388, 2009.

[2] W. J. McNeil, S. L. Bellinger, T. C. Unruh, E. L. Patterson, J. K. Shultis, and D. S. McGregor, "Perforated diode fabrication for neutron detection," *IEEE Nucl. Sci. Symp. Conf. Rec*. **6**, 3732-3735 (2006).

[3] D. S. McGregor, W. J. McNeil, S. L. Bellinger, T. C. Unruh, and J. K. Shultis, "Microstructured semiconductor neutron detectors," *Nucl. Instr. and Meth. A* **608**, 125-131 (2009).

[4] A. M. Conway, T. F. Wang, N. Deo, C. L. Cheung, and R. J. Nikolic, "Numerical simulations of pillar structured solid state thermal neutron detector: efficiency and gamma-ray discrimination," *IEEE Trans. Nucl. Sci.* **56**, 2802-2807 (2009).

[5] R. J. Nikolic, A. M. Conway, C. E. Reinhardt, R. T. Graff, T. F. Wang, N. Deo, and C. L. Cheung, "Pillar structured thermal neutron detector with 6:1 aspect ratio," *Appl. Phys. Lett.* ***93***, 133502 (2008).

[6] Q. Shao, R. P. Radev, A. M. Conway, L. F. Voss, T. F. Wang, R. J. Nikolic, N. Deo, and C. L. Cheung, "Gamma-ray discrimination in pillar structured thermal neutron detectors," *Proc. SPIE* **8358**, 83581N (2012).

[7] Q. Shao, L. F. Voss, A. M. Conway, R. J. Nikolic, M. A. Dar, and C. L. Cheung, "High aspect ratio composite structures with 48.5% thermal neutron detection efficiency," *Appl. Phys. Lett.* **102**, 063505 (2013).

[8] T. W. Crane and M. P. Baker, Chapter 13 "Neutron Detectors," *Passive Nondestructive Assay of Nuclear Materials,* Doug Reilly, Norbert Ensslin, Hastings Smith Jr, and Sarah Kreine, eds, (US Nuclear Regulatory Commission, 1991).

[9] G. F. Knoll, *Radiation Detection and Measurement*, 3rd ed. (*Wiley*, New York, 2000).

[10] J. W. Murphy, G. R. Kunnen, I. Mejia, M. A. Quevedo-Lopez, D. Allee, and B. Gnade, "Optimizing diode thickness for thin-film solid state thermal neutron detectors,"*Appl. Phys. Lett.* **101**, 143506 (2012).

[11] N. Deo, J. R. Brewer, C. E. Reinhardt, R. J. Nikolic, and C. L. Cheung, "Conformal filling of silicon micro-pillar platform with 10boron," *J. Vac. Sci. Tchnol. B* **26**, 1309-1314 (2008).

[12] American National Standard for Evaluation and Performance of Radiation Detection Portal Monitors for Use in Homeland Security. Technical Report. ANSI 42.35-2006, American Nuclear Standards Institute, Washington, D. C.

[13] R. T. Kouzes, J. R. Ely, A. T. Lintereur, and D. L. Stephens, "Neutron detector gamma-ray insensitivity criteria," PNNL-18903 (2009).

[14] K. –C. Huang, R. Dahal, J. J. –Q. Lu, A. Weltz, Y. Danon, and I. B. Bhat, "Scalable large-area solid-state neutron detector with continuous p-n junction and extremely low leakage current," *Nucl. Instr. and Meth. A* **763**, 260-265 (2014).

[15] K. –C. Huang, R. Dahal, J. J. –Q. Lu, Y. Danon, and I. B. Bhat, "High detection efficiency micro-structured solid-state neutron detector with extremely low leakage current fabricated with continuous p-n junction," *Appl. Phys. Lett.* **102**, 152107 (2013).

[16] R. Dahal, K. C. Huang, J. Clinton, N. LiCausi, J. –Q. Lu, Y. Danon, and I. Bhat, "Self-powered micro-structured solid state neutron detector with very low leakage current and high efficiency," *Appl. Phys. Lett.* **100**, 243507 (2012).

[17] S. L. Bellinger, R. G. Fronk, W. J. McNeil, T. J. Sobering, and D. S. McGregor, "Improved high efficiency stacked microstructured neutron detectors backfilled with nanoparticle ^{6}LiF," *IEEE Trans. Nucl. Sci.* **59**, 167-173 (2012).